

# A Fine Evaluation Method for Cube Copying Test for Early Detection of Alzheimer’s Disease

Xinyu Jiang<sup>1</sup>, Cuiyun Gao<sup>1\*</sup>, Wenda Huang<sup>1</sup>, Yiyang Jiang<sup>1</sup>, Binwen Luo<sup>1</sup>, Yuxin Jiang<sup>1</sup>

Mengting Wang<sup>1</sup>, Haoran Wen<sup>1</sup>, Yang Zhao<sup>1</sup>, Xuemei Chen<sup>2</sup>, Songqun Huang<sup>3</sup>

<sup>1</sup>General Purposed Auto-Test & AI Tech. Lab, Anhui Jianzhu University, Hefei, 230601, China

<sup>2</sup>Hefei Smart Healthcare Center & Apartment for Elderly, Hefei Industrial Investment Co., LTD  
Hefei, 230011, China

<sup>3</sup>Department of Cardiovasology Changhai Hospital, Second Military Medical University,  
Shanghai, 200433, China

## Abstract:

Background: Impairment of visual spatial cognitive function is the most common early clinical manifestation of Alzheimer’s Disease (AD). When the Montreal Cognitive Assessment (MoCA) uses the “0/1” binary method (“pass/fail”) to evaluate the visual spatial cognitive ability represented by the Cube Copying Test(CCT), the elder with less formal education generally score 0 point, resulting in serious bias in the evaluation results. Therefore, this study proposes a fine evaluation method for CCT based on dynamic handwriting feature extraction of DH-SCSM-BLA.

method : The Cogni-CareV3.0 software independently developed by our team was used to collect dynamic handwriting data of CCT. Then, the spatial and motion features of segmented dynamic handwriting were extracted, and feature matrix with unequal dimensions were normalized. Finally, a bidirectional long short-term memory network model combined with attention mechanism (BiLSTM-Attention) was adopted for classification.

Result: The experimental results showed that: The proposed method has significant superiority compared to similar studies, with a classification accuracy of 86.69%. The distribution of cube drawing ability scores has significant regularity for three aspects such as MCI patients and healthy control group, age, and levels of education. It was also found that score for each cognitive task including cube drawing ability score is negatively correlated with age. Score for each cognitive task including cube drawing ability score, but positively correlated with levels of education significantly. Conclusion: This study provides a relatively objective and comprehensive evaluation method for early screening and personalized intervention of visual spatial cognitive impairment.

**Keywords:** cube copying test; visuospatial cognitive ability; DH-SCSM-BLA; Spatial features; Motion features; BiLSTM-Attention

## 1. Introduction

### 1.1 Background

Alzheimer’s Disease (AD) is a neurodegenerative disorder characterized by insidious onset and progressive development, which affects memory, thinking, and the ability to perform daily activities[1],[2]. It is estimated that 15.07 million people aged

---

\* Corresponding author.

E-mail addresses: jiangxinyu@stu.ahjzu.edu.cn (X. Jiang), gaocuiyun@ahjzu.edu.cn (C. Gao)

60 years or older in China have dementia: 9.83 million with Alzheimer's disease[3]. The number of people with dementia is projected to increase from 57.4 million cases globally in 2019 to 152.8 million cases in 2050[4]. Moreover, the low consultation rate among AD patients is primarily due to a lack of attention in the early stages of the disease. Consequently, many patients do not seek medical care until the condition has progressed to later phases, often missing the optimal window for intervention. Therefore, the management of AD must be guided by the principle of early detection and timely intervention. The early stage of the condition, known as Mild Cognitive Impairment (MCI), represents a transitional stage between being cognitively unimpaired and dementia, so consensus has been reached to focus primary interventions in this population to prevent dementia[3]. One of the most prominent early signs in MCI is the decline in cognitive function. Cognitive impairment affects skills such as communication, comprehension, or memory, handwriting is one of the daily activities affected by these kinds of impairments, and its anomalies are already used as diagnosis sign. Nowadays, many studies have been conducted to investigate how cognitive impairments affect handwriting[5]. Research has found that motor planning and cognitive ability appear to be more closely related to handwriting[6]. When Alzheimer's disease was first diagnosed in 1970, researchers had already found a positive correlation was observed between the severity of the dementia and handwriting measures[7]. Further research has revealed that the pathological mechanisms of dysgraphia are closely associated with impaired visuospatial cognitive ability. Cube copying measures visuospatial cognitive ability, which is often impaired in Alzheimer's disease[8].

To systematically quantify cognitive impairments, clinicians have developed multidimensional assessment tools including the Mini-Mental State Examination (MMSE), Montreal Cognitive Assessment (MoCA), and Addenbrooke's Cognitive Examination-III (ACE-III). These tests, designed primarily for assessing AD and other dementia-causing conditions, focus predominantly on cognitive domains affected in these disorders: episodic memory, spatiotemporal orientation, language, and higher visual processing[9]-[12]. Recent years have witnessed growing emphasis on handwriting analysis-based cognitive evaluation methods. Studies demonstrate significant differences in handwriting characteristics, speed, rhythm, and stability between Parkinson's disease (PD) patients, AD patients, and healthy individuals[13],[14]. Therefore, this study primarily investigates the impact of handwriting feature analysis methods in the CCT on cognitive assessment, utilizing multiple AD-related cognitive scales.

## 1.2 Related Work

This section focuses on the core objective of assessing visuospatial cognitive ability. It begins by surveying research on dynamic handwriting signals, analyzing the current status of studies from three dimensions: evaluation methods for visuospatial cognitive ability, feature extraction and classification methods based on static images, and feature extraction and classification methods based on dynamic trajectories. The aim is to achieve an assessment of visuospatial cognitive ability using dynamic handwriting

signals.

### **1.2.1 Methods for assessing CCT based visuospatial cognitive ability**

Visuospatial cognitive ability, a core dimension of cognitive function, encompasses object position perception, spatial relationship judgment, and visual-motor coordination. It serves as an early biomarker for neurodegenerative disorders such as AD, Lewy body dementia (DLB), and PD, holding significant clinical diagnostic value. Salimi et al.[15] demonstrated that visuospatial assessment can effectively enhance diagnostic accuracy for Alzheimer’s disease, particularly during early disease stages, serving as a crucial supplementary tool for cognitive evaluation. CCT is a classic visuospatial cognitive ability assessment task and possesses unique diagnostic value. The CCT can also be viewed as a drawing process, which requires the integration of multiple cognitive resources to draw three-dimensional spatial figures, primarily involving visuospatial processing, eye-hand coordination, and other higher-order cognitive ability.

This process involves integrating multiple cognitive resources to construct three-dimensional spatial figures, primarily engaging visuospatial processing and hand-eye coordination—key advanced cognitive ability[16]. Shimada et al.[17] found that cube replication tasks are sensitive and effective neuropsychological tests, capable of revealing early visuospatial dysfunction and constructive apraxia in AD. Furthermore, the CCT has been incorporated into multiple standardized assessment scales. For instance, Sebastian Corral et al.[9] demonstrated that the MOCA scale quantifies visuospatial cognitive ability through a clock drawing task (3 scores) and a 3D cube copy task (1 scores). Andrew et al.[18] compared the diagnostic accuracy of ACE, ACE-R, and MMSE scales, finding that ACE-R evaluates visuospatial cognitive ability through cube replication with slightly better accuracy than MMSE. Additionally, Kazuya et al.[19] utilized subtests from the Visual Perception Function Scale (VOSP) – including cube/pentagon replication and clock drawing tasks – to assess visual perception abilities and investigate visual impairment characteristics in PD patients. Juan [20] employed the Rey-Osterrieth Complex Figure Test (ROCF) to assign quantitative scores based on geometric similarity between drawings and models, thereby evaluating participants’ visual memory and spatial organization abilities. However, traditional assessment methods fail to capture dynamic cognitive processes. With the rapid development of digital technologies, dynamic handwriting analysis has emerged as a novel technique for visuospatial evaluation. This approach has also been applied to CCT, where motion handwriting data collected during CCT completion can quantify spatial perception, directional judgment, and motor coordination ability, thereby extracting quantifiable features that effectively characterize visuospatial cognitive ability.

### **1.2.2 Feature extraction methods based on static images**

Feature extraction from static images aims to reduce the dimensionality of raw image data while preserving the most informative and discriminative features[21]. For cube copying images, this process involves extracting critical information including line structures, geometric shapes, and bending angles from the collected images to

support subsequent research. For instance, Bernardo et al.[22] applied Convolutional Neural Network (CNN) model as a feature extractor and a support vector machine (SVM) as a classifier to analyze differences between handmade drawings of PD patients and healthy subjects. Pakize et al.[23] proposed using 1D features from tasks in the public dataset DARWIN to generate 2D RGB image features, which were yielded into the novel CNN model for early AD diagnosis analysis. Additionally, Wahiba Ismaiel et al.[24] extracted edge features from original images using Canny edge detection and enhanced the recognition of static Arabic sign language gestures via ResNet50 and the Agile Convolutional Neural Network (ASLR\_CNN).

While static images are widely used, they cannot adequately capture temporal dynamics, limiting their effectiveness. This has positioned dynamic trajectory-based feature extraction as a key advancement, especially in fields like neurological disease assessment and behavior analysis, where the analysis of motion is crucial.

### 1.2.3 Feature extraction methods based on dynamic handwriting

Dynamic trajectories provide richer temporal information than static images, enabling more comprehensive analysis. Researchers extract relevant features from dynamic handwriting signals to provide crucial evidence for disease diagnosis and cognitive assessment. For instance, Nardone et al.[25] conducted independent analysis by integrating handwriting signals from multiple handwriting tasks, preserving fine motor information through stroke-by-stroke analysis to detect cognitive decline. Valla et al.[26] achieved efficient classification of PD patients by extracting kinematic and spatiotemporal features from drawing trajectories in the Archimedes spiral drawing test. Rios-Urrego et al.[27] systematically compared the modeling effects of three types of features—kinematic, geometric, and nonlinear dynamic features—on Parkinson’s writing disorders, achieving a maximum classification accuracy of 93.1%.

In dynamic handwriting research, deep learning models are predominantly integrated. Traditional machine learning methods primarily employ classifiers such as K-nearest neighbor (KNN), decision trees (DT), and random forests (RF) [26]-[29]. With the advancement of deep learning technologies, classification and prediction methods utilizing deep models—including CNN, bidirectional gated recurrent units (BiGRU), and long short-term memory networks (LSTM)—have emerged as key research focuses in this field [30]-[35]. For example, Ma et al.[28] proposes a novel spatial temporal spectral fusion neural network (STSNet), the model can efficiently fuse complementary information from static handwriting images and dynamic multi-sensory fusion signals for the fine-grained assessment of tremor severity in PD. Cilia et al.[29] constructed a novel online handwriting dataset to analyze combinations of handwriting features for AD diagnosis. They utilized multiple machine learning algorithms, including DT, RF, KNN, and Logistic Regression (LR), for AD classification. Wang et al.[30] demonstrated that 3D CNN models outperformed 1D, 2D, and 3D-CNN models in capturing spatiotemporal dynamics, providing new insights for designing deep learning architectures for handwriting classification. Diaz et al.[31] developed a CNN-BiGRU hybrid model to evaluate the potential of dynamic handwriting analysis in PD. Ma et al.[32] combined a novel Transformer-based deep learning model with

Archimedean spiral drawing tasks performed by patients and healthy subjects, effectively assessing its potential for diagnosing tremor symptoms. Vidhya R. [33] proposed integrating the feature extraction capabilities of ResNet with the temporal modeling advantages of LSTM, revealing the model's exceptional performance in identifying early AD biomarkers.

#### 1.2.4 Relative Research Foundations of Our Team

Since 2021, our team has been conducting research on early detection and intervention for Alzheimer's disease. Based on comprehensive study of scales such as the MMSE and MOCA, we have developed two cognitive assessment apps [36] and a web-based testing platform. All three software have the function of remote cognitive function testing and automatic uploading of test data to cloud server. Meanwhile, for intervention studies, our team developed a brain health exercise software and proposed a fuzzy progress evaluation method [37], while also designing training software for scenario-based object retrieval based on VR. The software developed by our team, named Cogni-Care (V1.0, V2.0, and V3.0), including a total of 11 tasks assessing short-term memory, executive function, naming, visuospatial cognition, calculation, attention, language ability, orientation, abstraction, and delayed memory. The visuospatial cognition task includes clock drawing test and cube copying test. The intelligent speech recognition for language assessment was implemented based on the Iflytek Automatic Speech Recognition (ASR) Package, and the assessment of the CCT task is conducted using an intelligent algorithm that was developed independently by our team.

During data collection, we found that most of participants aged over 70 had less formal education, who lacked the concept of solid geometry or three-dimensional (3D) and also lacked training in cube copying. As a result, the cube images they draw generally lacked 3D characteristics, which would make these people get nearly all zero scores when the scoring criteria of MoCA is strictly executed in the CCT, and lead to undermining the validity of visuospatial ability assessment. Therefore, our team introduced a fine scoring standard for CCT. This new criterion classifies drawings based on continuity, presence of two-dimensional (2D) features, and emergence of three-dimensional attributes, establishing a four-level scoring system (As described in Table 1). Furthermore, the team primarily analyzed static images of cube copying produced by participants, using an edge gradient-based contour extraction algorithm to assign scores. As mentioned before, dynamic trajectories provide richer temporal information than static images. Therefore, the current scoring method for cube copying ability based on static images urgently needs improvement.

In order to solve the above problems, this study proposes a fine assessment method for cube copying ability based on the DH-SCSM-BLA method. The main contributions are as follows:

(1) A fine scoring method was proposed to address the inaccuracy and incompleteness of the original MoCA cube copying test, which relies on a binary classification (0 or 1 scores).

(2) A Spatial-Cosine-Similarity & Motion (SCSM) feature extraction method based on dynamic handwriting segmentation is proposed, encompassing both spatial and

motion features of segmented trajectories;

(3) Comparative analyses of cube copying test scores are conducted from three perspectives (MCI patients vs. healthy controls, different age groups, and different educational levels), revealing significant discriminative patterns;

(4) Statistical significance analyses are performed between each cognitive indicator score of Cogni-CareV3.0 App (including the CCT visuospatial cognitive ability score) and two factors (age and educational level). The results indicated that all cognitive metric scores derived from the Cogni-CareV3.0 App are significantly negatively correlated with age, but significantly positively correlated with educational level.

## 2. Method

As shown in Fig. 1, the framework of the proposed method contains three modules: (1) Data modeling, (2) Feature extraction, (3) Classification recognition. The Cogni-CareV3.0 software independently developed by our team was used to collect dynamic handwriting data of CCT. Then, the spatial and motion features of segmented dynamic handwriting were extracted, and feature matrix with unequal dimensions were normalized. Finally, a bidirectional long short-term memory network model combined with attention mechanism (BiLSTM-Attention) was adopted for classification.

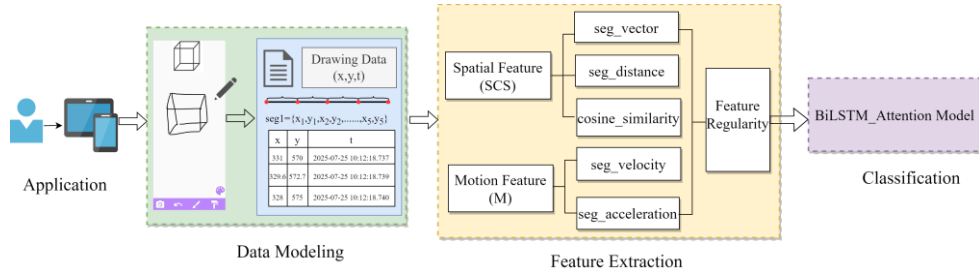


Fig.1. Block diagram of the proposed method

### 2.1 Handwriting data mathematical modeling

The dynamic handwriting of the cube copying is characterized by the coordinates  $(x,y)$  and time  $t$  as core parameters. The original handwriting trajectory dataset is defined as  $TR$ , where  $TR=[TR_1, TR_2, \dots, TR_k, \dots, TR_N]$ , with  $k$  denoting the test sample index and  $N$  the total number of test samples. Each sample  $TR_k$  consists of  $TR_k = [S_{k,1}, S_{k,2}, \dots, S_{k,i}, \dots, S_{k,L}]$ , where  $S_{k,i} = (x_{k,i}, y_{k,i}, t_{k,i})$ , with  $S_{k,i}$  denoting the coordinates and time values at the  $i$ -th moment of the  $k$ -th sample. The time  $t$  is measured in milliseconds, and  $L$  represents the handwriting length (number of handwriting points). Since the number of handwriting points in cubic trajectories varies across individuals,  $L$  is a variable, resulting in a data dimension of  $3L$  per sample.

The data acquisition and visualization of single-sample modeling are described as follows: participants complete the CCT using the Cogni-CareV3.0 App, which saves all handwriting information ( $TR$ ). Fig. 2 denotes the  $TR_k$  representation process, where the handwriting coordinates of a specific cube region are shown in the red box. The cube shape is reconstructed from the acquired handwriting data to visually demonstrate the modeling process. Different colored line segments in the figure are generated sequentially based on the timestamp of handwriting points, corresponding to



different drawing phases. The red arrows indicate the directions of the first and second strokes.

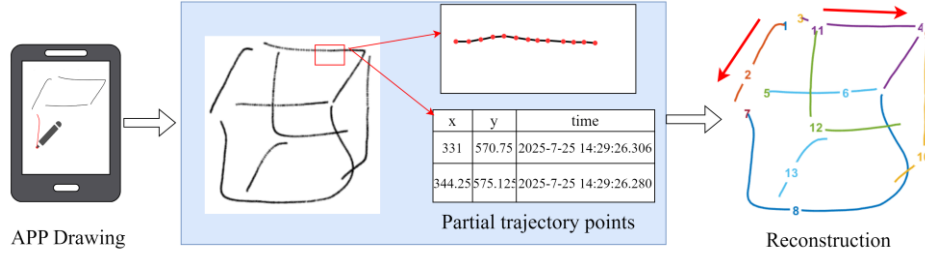


**Fig. 2.** the model of handwriting data

## 2.2 Feature extraction based on SCSM

The original handwriting trajectory data  $(x_k, y_k, t_k)$  are processed through a segmentation method to extract 12-dimensional spatial features and 2-dimensional motion features, denoted as SCS features and M features respectively. The SCS features include 10-dimensional segment coordinate vectors, 1-dimensional intra-segment distance, and 1-dimensional cosine similarity. The M features consist of 1-dimensional segment average velocity and 1-dimensional acceleration. These spatial and motion features are combined to form a 14-dimensional feature vector termed SCSM. The feature extraction process is denoted with the  $k$ -th sample  $TR_k$ .

### 2.2.1 Spatial features

The handwriting trajectory coordinates are segmented into fixed-length segments of 5 points, where consecutive segments are connected end-to-start and non-overlapping. Fig. 3 presents a schematic diagram of the handwriting trajectory coordinates. Specifically, Fig. 3(a) and Fig. 3(b) denote the coordinate relationships between segments and within a single segment, respectively.

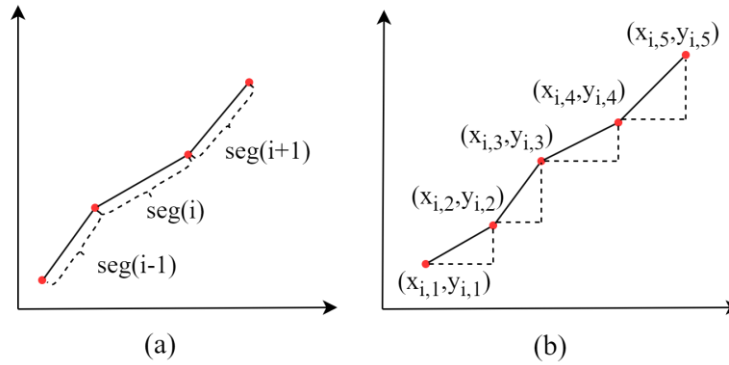


**Fig. 3.** Segment Coordinate diagram. (a) Inter-segment diagram, (b) Intra-segment diagram.

The segment vector ( $seg\_vector$ ) is obtained by converting the intra-segment coordinates into a 10-dimensional vector as shown in Fig.3(b),

$$seg_i = \{x_{i,1}, y_{i,1}, x_{i,2}, y_{i,2}, \dots, x_{i,5}, y_{i,5}\} \quad (1)$$

where  $i$  represents the segment index, and the numbers 1, 2, ..., 5 represent the indices of the coordinate points within the segment.

The sum of intra-segment distances ( $seg\_distance$ ) is the cumulative Euclidean

distance between all adjacent points within a single segment. The calculation formula for the intra-segment distance sum  $dis_i$  is:

$$dis_i = \sqrt{\sum_{j=1}^4 (x_{i,j+1} - x_{i,j})^2 + (y_{i,j+1} - y_{i,j})^2} \quad (2)$$

where  $(x_{i,j}, y_{i,j})$  denotes the coordinates of the  $j$ -th point in  $i$ -th segment ( $j=1,2,\dots,5$ ).

Cosine similarity (cos\_similarity) quantifies the directional consistency between trajectory segments by calculating the cosine value of the angle between them. A value closer to 1 indicates that the segments are aligned in the same direction, a value approaching 0 signifies perpendicular alignment, and a value near -1 denotes opposite directions. This method typically adopts vector space similarity metrics[38], and the inter-segment vector diagram is denoted in Fig. 4.

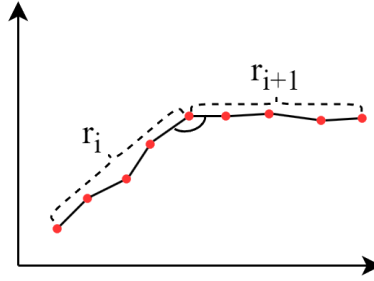


**Fig. 4.** Inter-segment Angle diagram

Given two adjacent segment vectors  $r_i = \{x_{i,1}, y_{i,1}, \dots, x_{i,5}, y_{i,5}\}$  and  $r_{i+1} = \{x_{i+1,1}, y_{i+1,1}, \dots, x_{i+1,5}, y_{i+1,5}\}$ , the inter-segment cosine similarity feature vector  $sim$  can be obtained as follows:

$$sim = \frac{r_i \cdot r_{i+1}}{\|r_i\| \|r_{i+1}\|} = \frac{\sum_{j=1}^5 (x_{i,j} \cdot x_{i+1,j} + y_{i,j} \cdot y_{i+1,j})}{\sqrt{\sum_{j=1}^5 (x_{i,j}^2 + y_{i,j}^2)} \cdot \sqrt{\sum_{j=1}^5 (x_{i+1,j}^2 + y_{i+1,j}^2)}} \quad (3)$$

where  $r_i \cdot r_{i+1}$  denotes the dot product of two segment vectors, while  $\|r_i\|$  and  $\|r_{i+1}\|$  represent their respective magnitudes.

### 2.2.2 Motion features

Motion features include the average velocity and acceleration. Segment velocity can measure the speed of handwriting point movement, and the average segment velocity  $v_i$  can be obtained using the intra-segment distance sum  $dis_i$  calculated by Equation (2):

$$v_i = \frac{dis_i}{\Delta t_i} \quad (4)$$

where the intra-segment time difference  $\Delta t_i = t_{i,end} - t_{i,start}$ , where  $t_{i,end}$  represents the time of the last point in the current  $i$ -th segment, and  $t_{i,start}$  denotes the time of the first point in the same segment.

Segment acceleration can capture sudden changes in handwriting velocity. It is derived by calculating the velocities of adjacent points within the segment and their



corresponding time intervals, with the expression for segment acceleration  $a_i$  given by:

$$a_i = \frac{v_{i,j+1} - v_{i,j-1}}{t_{i,j+1} - t_{i,j-1}} \quad (5)$$

where  $v_{i,j+1}$  and  $v_{i,j-1}$  represent the instantaneous velocities of the  $(j+1)$  and  $(j-1)$  points in the  $i$ -th segment of the  $k$ -th sample, while  $t_{i,j+1}$  and  $t_{i,j-1}$  denote the timestamps of the coordinate points ( $j=2,3,4$ ).

### 2.2.3 Feature Normalization

The five aforementioned features are concatenated into a composite feature  $f$  according to Equation (6). However, this concatenation method has a limitation: since the original handwriting sequence  $L$  varies in length across samples, the number of segments obtained after segmentation also differs per sample. Meanwhile, the feature dimension extracted from each segment remains fixed—resulting in composite features of unequal lengths and thus forming feature vectors with non-uniform dimensions. To address this issue, this paper achieves feature dimension unification through standardized length intervals and resampling. The specific operations are as follows: A fixed-length interval of  $[14, L_{std}]$  is established for the standardized handwriting sequence. Here, 14 is the intrinsic dimension of the feature, and  $L_{std}$  is the standardized sequence length, dictated by the mean length of the sample sequences. Resampling is then performed on the original sequence  $L$ : if  $L < L_{std}$  the sequence is extended via interpolation; if  $L > L_{std}$  it is compressed through downsampling. After these processes, the feature set of all samples is expressed as shown in Equation (7):

$$f = [seg, dis, sim, v, a]_{14 \times L_{std}} \quad (6)$$

$$F = \begin{bmatrix} f_1 \\ f_2 \\ \vdots \\ f_N \end{bmatrix} \quad (7)$$

where  $f_1, f_2, \dots, f_N$  represent the extracted features of the 1st, 2nd, ..., and  $N$ th samples after normalization, and each  $f_d (d=1,2,\dots,N)$  is a feature matrix with dimension of  $14 \times L_{std}$ .

## 2.3 Classification based on BiLSTM-Attention

For the extracted feature vectors, this study adopts a bidirectional long short-term memory network model (BiLSTM-Attention) for classification. Initially proposed by Zhou et al. [39] for natural language processing tasks, this model integrates bidirectional long short-term memory (BiLSTM) with an attention mechanism, enabling effective capture of critical information from sequential features. This paper combines the previously proposed features to obtain 3 combined features, namely SCS, M, and SCSM features. SCS include segment coordinates, segment distance, and inter-segment

cosine similarity; M combines segment velocity and acceleration; and SCSM merges the first two types of features. Each combined feature is input into the BiLSTM-Attention model for classification, with the optimal feature combination identified through evaluation of classification accuracy.

The network model designed in this paper (Fig. 5) comprises an input layer, a bidirectional LSTM layer, an attention layer, and an output layer. The specific workflow is as follows: The input layer receives a standardized feature sequence  $F=[F_1, F_2, \dots, F_t, \dots, F_n]$  (where  $n$  denotes the dimension of sample features) and feeds it into a two-layer LSTM. The bidirectional LSTM layer processes the original feature sequence through a forward layer and the reversed feature sequence through a backward layer. Outputs from the two layers are concatenated to generate a hidden layer state matrix  $H=[h_1, h_2, \dots, h_t, \dots, h_n]$  (where  $h_t$  represents the bidirectional hidden state at time step  $t$ ,  $i$  denotes the hidden layer dimension of the LSTM neurons set to 128, and  $C_t$  and  $h_t$  respectively denote the cell state and hidden state of the LSTM at time step  $t$ ). This matrix serves as the input to the attention layer, whose core mechanism computes the weight relationships between “query (Q), key (K), and value (V)” [40]. The layer first performs linear transformations on  $H$  to obtain Q, K, and V. Subsequently, the SoftMax layer calculates the attention weight for each time step using Scaled Dot-Product Attention, followed by a linear mapping to generate the intermediate output. The output layer employs regularization to mitigate overfitting, and the features are mapped to the category space via a fully connected layer to produce the final classification result.

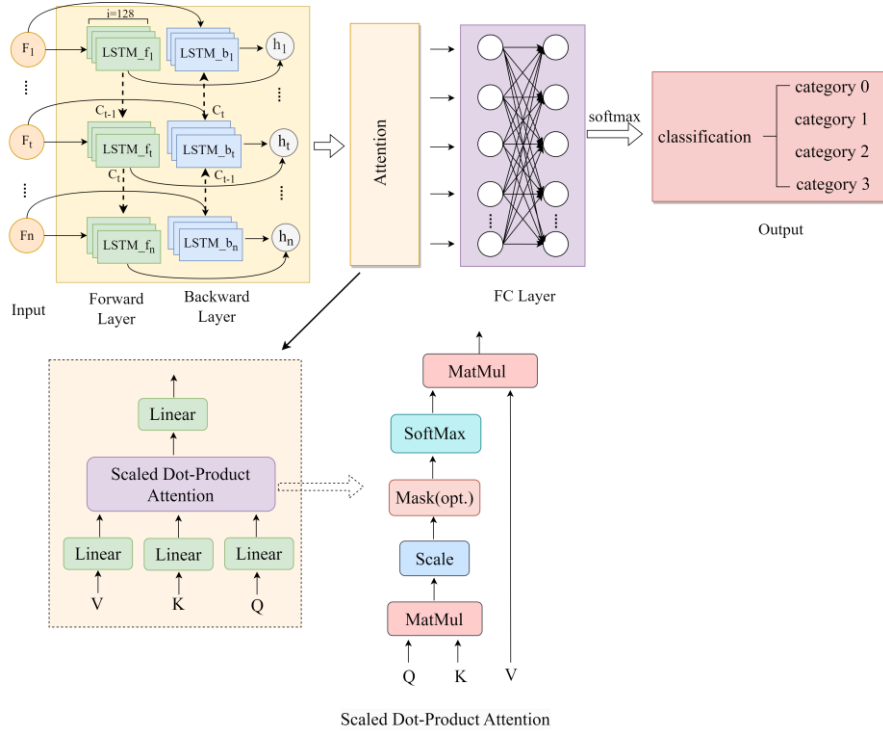


Fig. 5. BiLSTM-Attention network structure

### 3. Experiment and result

This study adheres to the principles of academic ethics: the personal information

of all participants is strictly confidential, and data collection was conducted with the informed consent of the subjects.

The Cogni-CareV3.0 App collects comprehensive test data through its ten task modules, namely short-term memory, executive function, naming animals, visuospatial cognition, calculation, attention, language, abstract, delayed memory and orientation, where the visuospatial module mainly includes the CCT and clock recognition. Data were collected from participants recruited from a nursing home, a village, and a university. All subjects completed the full set of game-based tests using the Cogni-CareV3.0, forming a self-collected dataset comprising 224 participants. The gender ratio, age distribution, and educational background of the participants are presented in Fig. 6(a), 6(b), and 6(c), respectively, while the distribution of participants MCI and Healthy Control is denoted in Fig. 6(d).

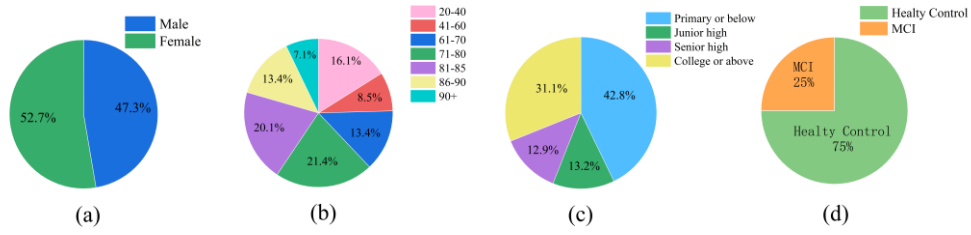


**Fig. 6.** Distribution of participants' information. (a) Distribution of Sex; (b) Distribution of Age; (c) Distribution of Educational Level; (d) Distribution of MCI and Healthy Control.

### 3.1 Acquisition of handwriting data

As previously described, the study utilized handwriting data from the visuospatial task of the selected dataset to evaluate the potential of dynamic handwriting features in AD-related visuospatial cognition. The CCT in the Cogni-CareV3.0 App is denoted in Fig. 7, where participants draw standard cubes on the game interface, with their handwriting data being stored in real-time in the database.

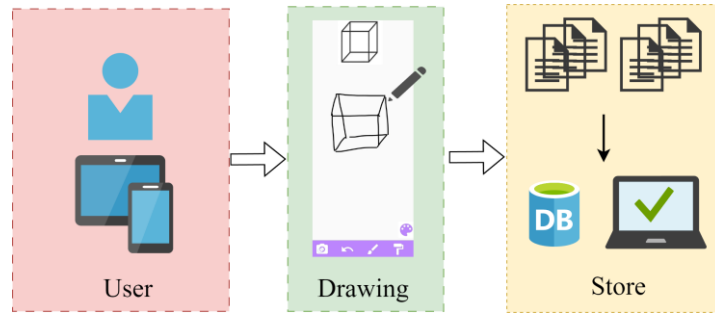


**Fig. 7.** Block diagram of handwriting data acquisition

### 3.2 Fine scoring criteria for CCT

As mentioned earlier, the elder with lower educational level generally score 0 point based on the scoring criteria for visuospatial tasks in the MOCA. Therefore, in this study, sample labels are defined based on the accuracy and structural integrity of the drawings completed by participants during the CCT, and the data were categorized into four levels: Category 0 (0 score), Category 1 (1 score), Category 2 (2 score), and Category 3 (3 score). The specific classification rules are detailed in Table 1.

**Table 1.** Classification Rules

Category	Description
0 score	Unable to form a two-dimensional structure, only partial lines, scattered line segments, or a circle, a randomly smeared black blob, etc. can be drawn.
1 score	The drawn figures have 2D structural characteristics and no 3D stereoscopic structure, such as only one or more unconnected rectangles being drawn.
2 score	Able to draw a cube with multiple surfaces; relatively complete shape, basic 3D cube structure, slight proportional imbalance, or 1-2 missing edge lines.
3 score	Requires 12 edge lines fully drawn, correct vertex connections, complete structure, clear lines, distinct cubic spatial structure, and no obvious deformation.

All samples in the current dataset were classified according to the four-level classification criteria in Table 1. The training set, validation set, and test set were divided in a 8:1:1 ratio (Table 2).

**Table 2.** Number of Sample Categories

Data	Total	Category 0	Category 1	Category 2	Category 3
Total set	224	48	67	67	42
Training set	178	38	53	53	34
Validate set	23	5	7	7	4
Test set	23	5	7	7	4

### 3.3 Results analysis

The experiments were conducted on a server equipped with NVIDIA RTX A4000 GPU and Intel processors (Table 3), with the operating environment based on the PyTorch 2.0.0 + CUDA 11.8 framework.

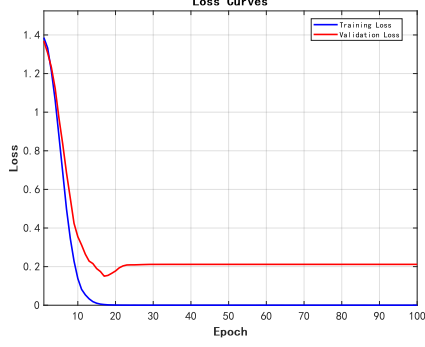
**Table 3.** Environment parameter

	Component	Version
Hardware	GPU	NVIDIA RTX A4000 GPU(16GB)
	CPU	Intel Xeon(R) W-2223 CPU
	GPU memory	32GB
	OS	Windows 10
Software	Python	Python3.9
	Pytorch	2.0.0

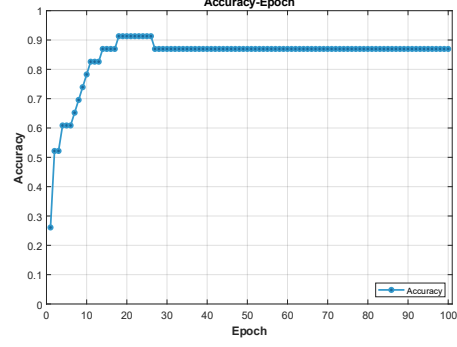
Under the aforementioned experimental conditions, the training set comprised 178 dynamic handwriting samples, where the input feature is defined as  $F$ . Given the small scale of the dataset, a 5-fold cross-validation method was employed to evaluate the model’s generalization performance. This study evaluates the performance of the classification method using three metrics: Accuracy, Precision, and F1 score. As presented in Table 4, experimental results indicate that Experiment 3 achieved the optimal performance. The model reached a stable performance state after 30 epochs. Notably, the maximum performance is achieved with the optimal configuration, where the number of LSTM layers, hidden layer dimension, attention layer input dimension, and learning rate are set to 2, 128, 256, and 0.005, respectively.

**Table 4.** BiLSTM-Attention Model Parameters

Number	LSTM Layer	Hide_dim	Attention_dim	Lr	Epoch	Accuracy/%	Expense/s
1	2	64	128	0.005	100	78.26	2.48
2	2	128	256	0.001	100	82.61	2.80
3	2	128	256	0.005	100	86.96	2.88
4	2	128	256	0.01	100	82.61	3.09
5	1	128	256	0.005	100	78.26	2.71



(a)



(b)

**Fig. 8.** Loss and Accuracy Curves of BiLSTM-Attention Model. (a) Loss Curves , (b) Accuracy Curves.

To avoid limitations of single classification methods and comprehensively evaluate model performance, this study compares the recognition performance of multiple classifiers on the feature SCSM, including GRU, BiGRU, and Transformer models. Table 5 presents the classification performance of the feature across different models, with core metrics such as accuracy, precision, and F1 score used for evaluation.

**Table 5.** Accuracy of different classification algorithms

Model	Accuracy(%)	Precision(%)	F1 score
RF	69.57	70.79	0.692
DT	60.29	60.55	0.602
KNN	47.83	51.45	0.452
DNN	83.33	84.49	0.822
Transformer	73.91	73.91	0.737
BiGRU	82.61	84.96	0.822
GRU	69.57	71.62	0.698
LSTM	73.91	75.36	0.738
LSTM-Attention	78.26	78.41	0.780
BiLSTM	73.91	75.54	0.743
BiLSTM-Attention	86.96	88.37	0.866

Given the limited sample size of the dataset, we initially selected GRU and BiGRU models—both designed for small sample learning—as baseline benchmarks. However, the experimental results revealed that the BiLSTM-Attention model achieved the highest classification accuracy.

The three obtained combined features, namely SCS, M, and SCSM were input into the BiLSTM-Attention model for ablation experiments. The classification results of these features on the dataset (as shown in Table 6) demonstrate that the SCSM combination feature achieves higher recognition accuracy than individual features.

**Table 6.** Comparison of feature ablation experiments

Feature Set	Dimension	Accuracy(%)	Precision(%)	F1 score
SCS	12	63.24	64.05	0.634
M	2	47.83	44.93	0.438
SCSM	14	86.96	88.37	0.866

## 4. Discussion

This study demonstrates the advantages of segmented feature extraction methods in evaluating visuospatial cognitive ability through dynamic handwriting analysis by comparing feature combinations with models. Building on this foundation, this chapter explores three key aspects: validating the effectiveness of segmented feature extraction, examining the distribution of visuospatial cognitive scores across different population groups, and conducting significance analysis of age and educational level effects on visuospatial cognitive performance.

### 4.1 Comparison between DH-SCSM-BLA method and similar

#### literature

To comprehensively evaluate the effectiveness of the proposed segmented feature extraction method, we selected methods from reference [26] and [27] as baseline benchmarks. Both studies focused on analyzing writing behaviors in neurological disorders, employing kinematic features for modeling. Notably, reference [27] further integrated geometric and nonlinear dynamics approaches to construct feature models, achieving classification performance for both PD patients and healthy individuals.

Since the extraction of geometric features (such as altitude\_diff, azimuth\_diff, and other parameters) usually relies on specific devices like digital tablets, while the data conditions of this study cannot directly obtain such features, to ensure the fairness and feasibility of the comparison, only directly extractable kinematic features (including curvature, writing speed, average acceleration) and nonlinear dynamic features (including sample entropy, Hurst index, correlation dimension) were selected for comparison. The experimental results are shown in Table 8.

**Table 7.** Feature Method Description

Feature	Name	Description
Kinem	curvature	The curvature of the local path
	speed	Changes in motion speed
	total_time	Total time of the path
	total_distance	Total distance
	Basic Statistical Features	Statistical characteristics of speed and acceleration, such as standard deviation, maximum and minimum values, and mean
	Peak speed	Indicates speed fluctuation
NLD	Acceleration peak	Indicates acceleration fluctuation
	Sample entropy	Trace the irregularity of the sequence
	Hurst	Track handwriting sequence persistence or anti-persistence
	Correlation Dimension	The complexity of system dynamics



**Table 8.** Experimental Results

	Model	Accuracy(%)	Precision(%)	F1 score
Method of [27]	BiLSTM-Attention	65.22	65.60	0.625
	RF	56.52	57.25	0.523
Method of [26]	BiLSTM-Attention	52.17	55.60	0.502
	RF	60.87	63.77	0.592
DH-SCSM-BLA	BiLSTM-Attention	86.96	88.37	0.866
	RF	69.57	70.79	0.692

As shown in Table 8, our proposed method was compared with the feature extraction approaches from reference [26] and reference [27] on the same dataset. To eliminate the interference of different classifiers, ablation experiments were conducted using the same model for both training and testing. The results demonstrate that our method outperforms the baselines across all evaluation metrics, which highlights the superior data representation capability of our SCSM feature extraction approach. For the relatively simple features proposed in reference [26], the RF model achieved better performance, as the complex BiLSTM-Attention model may suffer from performance degradation due to overfitting.

Valla et al.[26] extract kinematic and spatiotemporal features of handwriting trajectories but fail to capture local motion information. While the method proposed by Rios-Urrego et al.[27] captures the basic physical attributes of writing movements and the irregularities of time series, it loses the original spatial position (x, y) information of the sequence data and does not consider the trajectory trends within the time period. In contrast, the SCSM feature extraction method proposed in this paper focuses on the spatial morphological information of (x,y,t) sequences. Specifically, the SCSM method introduces a “segmented trajectory” strategy to quantify the continuity of trajectory motion.

## 4.2 Distribution of CCT Scores Among Different Groups

To further examine the distribution characteristics of visuospatial cognitive scores across populations, we analyzed the module’s distribution from three perspectives—MCI versus Healthy Control, age, and educational level—based on cognitive test scores (0-3 scores), as shown in Fig. 9.

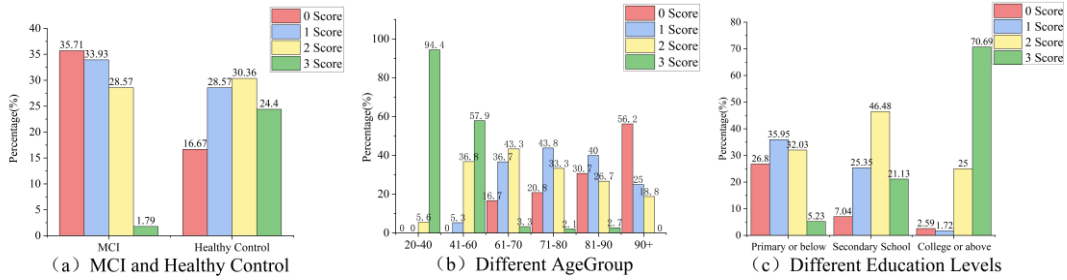


**Fig. 9.** Distribution of CCT scores across different groups.(a) Distribution of MCI and Healthy Control. (b) Distribution of Different Age Group. (c) Distribution of Different Educational Levels.

As shown in Fig. 9(a), the Healthy Control group exhibits a relatively balanced and

high-scoring distribution in the visuospatial task, while the MCI group shows a distinct low-scoring tendency—with 69.64% of participants scoring 0 or 1 score. This indicates that the cube-drawing visuospatial task is particularly sensitive to MCI, as individuals with MCI exhibit greater difficulties in this task compared to cognitively normal counterparts. Fig. 9(b) presents age-specific scores distribution patterns: task scores begin to decline in the 41–60 age group, with the rate of 3-scores dropping to 3.3% in the 61–70 age group. Collectively, these findings confirm a consistent downward trend in task performance across successive age groups. Fig. 9(c) highlights notable differences in task performance by educational level: individuals with lower educational level predominantly achieved low scores, reflecting limited cube-drawing proficiency, while middle school graduates exhibited relatively consistent performance. Notably, over 70% of university-educated participants successfully completed the task, suggesting that higher education may significantly enhance spatial visualization and expression skills—potentially through coursework in geometry, cartography, and engineering-related disciplines.

### 4.3 Significance Analysis On Scores of Each Cognitive Task

This study conducted significance analysis on scores of each cognitive task to age and educational level respectively. The Pearson correlation coefficient was calculated using the covariance matrix of data to evaluate the relationship strength between the two variables[41]. Based on the population distribution characteristics, the educational level was quantified as years of education for Pearson correlation coefficient.

As shown in Tables 9 and 10, there is a significant negative correlation between scores of each cognitive task and participants' age, where elder participants demonstrated lower cognitive scores. Conversely, scores of each cognitive task except Delayed Recall task showed a positive correlation with levels of education.

**Table 9.** Significance Analysis On Scores of Each Cognitive Task and Age

Task	Name	r-value	P-value	Significance
Task1	Short-term Memory	-0.523	<0.001	***
Task2	Trail Making	-0.608	<0.001	***
Task3	Naming animals	-0.361	<0.001	***
Task4	Clock	-0.405	<0.001	***
Task5	Cube Copy Test	-0.708	<0.001	***
Task6	Calculation	-0.573	<0.001	***
Task7	Attention	-0.633	<0.001	***
Task8	Language	-0.426	<0.001	***
Task9	Abstract	-0.555	<0.001	***
Task10	Delayed Recall	-0.486	<0.001	***
Task11	Orientation	-0.522	<0.001	***

Note: \*\*\*:  $p < 0.001$  (extremely significant), \*\*:  $p < 0.01$  (highly significant), \*:  $p < 0.05$  (significant), “-” indicates no statistical significance;  $|r| \geq 0.7$  indicates strong correlation,  $0.3 \leq |r| < 0.7$  indicates moderate correlation, and  $|r| < 0.3$  indicates weak correlation.

**Table 10.** Significance Analysis On Scores of Each Cognitive Task and Educational level

Task	Name	r-value	P-value	Significance
Task1	Short-term Memory	0.358	<0.001	***
Task2	Trail Making	0.398	<0.001	***
Task3	Naming animals	0.168	0.0122	*
Task4	Clock	0.344	<0.001	***
Task5	Cube Copy Test	0.537	<0.001	***
Task6	Calculation	0.343	<0.001	***
Task7	Attention	0.286	<0.001	***
Task8	Language	0.405	<0.001	***
Task9	Abstract	0.307	<0.001	***
Task10	Delayed Recall	0.109	0.1031	-
Task11	Orientation	0.372	<0.001	***

Note: Same as Table 9.

Furthermore, when performing significance analyses on cognitive task scores across different age groups and educational levels, the results of the significance analysis on scores of the cognitive task were found to be highest in the CCT.

## 5. Conclusion

In this study, we used a self-developed Cogni-CareV3.0 App to collect handwriting data and organized it into a dynamic handwriting dataset. To effectively preserve the spatiotemporal characteristics of original trajectories, we propose a fine assessment method which named DH-SCSM-BLA based on dynamic trajectories. This method constructs segmental feature combinations of trajectories using a “segmentation strategy” and normalizes them into equal-dimensional feature matrices, which are then input into a BiLSTM-Attention model. Experimental results demonstrate that the method achieved recognition rates of 86.69%, exhibiting superior classification performance compared to single-feature extraction methods. Collectively, this study provides a novel approach for the early screening of MCI.

However, this study has certain limitations. As discussed earlier, the CCT may be influenced by participants’ educational level: specifically, participants with lower years of education tend to receive 0 score, while those with higher education may generally obtain higher scores due to their prior training and experience related to geometric figures. As reported by Galaz et al.[42], the pentagon copying test can be used to quantify cognitive decline, which may mitigate the impact of 3D geometric figures on participants. In future research, supplementary assessment tools such as the pentagon copying test could be incorporated to conduct a comprehensive analysis of participants’ visuospatial cognitive abilities, thereby reducing the interference of educational background as a confounding variable on the evaluation results.

## 6. Acknowledgments

This study was financially supported by: (1) Key project of Natural Science funded by Education Department of Anhui Province of 2019 (KJ2019ZD56), China. (2) Clinical New Technology Incubation Project of Changhai Hospital (2024XC108), China. We thank iFlytek for its technical support and free resources, and also thank the

elderly residents at a nursing home and in a rural community for their strong support and assistance, as well as the nursing home staff for their significant coordination, which greatly facilitated the smooth progress of the research.

## References

- [1].Q. Wang, F. Gao, L. Dai, J. Zhang, D. Bi, Yong Shen, Clinical Research Investigating Alzheimer's Disease in China: Current Status and Future Perspectives Toward Prevention, The Journal of Prevention of Alzheimer's Disease, Volume 9, Issue 3, 2022, Pages 532-541, ISSN 2274-5807, <https://doi.org/10.14283/jpad.2022.46>.
- [2].World Health Organization, 31 March 2025, <https://www.who.int/ru/news-room/fact-sheets/detail/dementia>.
- [3].Jia L, Du Y, Chu L, et al. Prevalence, risk factors, and management of dementia and mild cognitive impairment in adults aged 60 years or older in China: a cross-sectional study. *Lancet Public Health*. 2020;5(12):e661-e671. doi:10.1016/S2468-2667(20)30185-7.
- [4].Emma Nichols, Jaimie D Steinmetz, Stein Emil Vollset, Estimation of the global prevalence of dementia in 2019 and forecasted prevalence in 2050: an analysis for the Global Burden of Disease Study 2019, The Lancet Public Health, Volume 7, Issue 2,2022,Pages e105-e125,ISSN 2468-2667, [https://doi.org/10.1016/S2468-2667\(21\)00249-8](https://doi.org/10.1016/S2468-2667(21)00249-8).
- [5].Cilia N D, Stefano C D, Fontanella F, et al. Using Handwriting Features to Characterize Cognitive Impairment[C]//2019.DOI:10.1007/978-3-030-30645-8\_62.
- [6].Tseng M H, Cermak S A . The Influence of Ergonomic Factors and Perceptual-Motor Abilities on Handwriting Performance[J].*American Journal of Occupational Therapy Official Publication of the American Occupational Therapy Association*,1993, 47(10):919-26.DOI:10.5014/ajot.47.10.919.
- [7].Jany Lambert, Bénédicte Giffard, Florence Nore, Vincent de la Sayette, Florence Pasquier, Francis Eustache, Central and Peripheral Agraphia in Alzheimer's Disease: From the Case of Auguste D. to a Cognitive Neuropsychology Approach, *Cortex*, Volume 43, Issue 7,2007,Pages 935-951, ISSN 0010-9452,[https://doi.org/10.1016/S0010-9452\(08\)70692-0](https://doi.org/10.1016/S0010-9452(08)70692-0).
- [8].Sebastian Palmqvist, Oskar Hansson, Lennart Minthon, Elisabet Londos, P3-168: The usefulness of cube copying for evaluating treatment of Alzheimer's disease, *Alzheimer's & Dementia*, Volume 4, Issue 4, Supplement, 2008, Page T569, ISSN 1552-5260,<https://doi.org/10.1016/j.jalz.2008.05.1734>.
- [9].Sebastian Corral, Pablo A. Gaspar, Rolando I. Castillo-Passi, Rocío Mayol Troncoso, Adrian P. Mundt, Yuriy Ignatyev, Rodrigo R. Nieto, Alicia Figueroa-Muñoz, Montreal Cognitive Assessment (MoCA) as a screening tool for cognitive impairment in early stages of psychosis, *Schizophrenia Research: Cognition*, Volume 36,2024,100302,ISSN 2215-0013,<https://doi.org/10.1016/j.scog.2024.100302>.
- [10].Said Dahbour, Maha Hashim, Ahmad Alhyasat, Anas Salameh, Abdallah Qtaishat, Ruba Braik, Touleen Mufeed Awni Alnimer, Mini-mental state examination (MMSE) scores in elderly Jordanian population, *Cerebral Circulation - Cognition and Behavior*, Volume 2,2021,100016,ISSN 2666-2450,<https://doi.org/10.1016/j.cccb.2021.100016>.
- [11].M. Gaete, S. Jorquera, S. Bello-Lepe, Y.M. Mendoza, M. Véliz, M.F. Alonso-Sanchez, J. Lira, Standardised results of the Montreal Cognitive Assessment (MoCA) for neurocognitive screening

- in a Chilean population, *Neurología (English Edition)*, Volume 38, Issue 4, 2023, Pages 246-255, ISSN 2173-5808, <https://doi.org/10.1016/j.nrleng.2020.08.021>.
- [12]. Aysha Mohamed Rafik Patel, Gina Gilpin, Anna Koniotes, Catherine Warren, Cian Xu, Paul W. Burgess, Dennis Chan, Clinic evaluation of cognitive impairment in post-COVID syndrome: Performance on legacy pen-and-paper and new digital cognitive tests, *Brain, Behavior, & Immunity - Health*, Volume 43, 2025, 100917, ISSN 2666-3546, <https://doi.org/10.1016/j.bbih.2024.100917>.
- [13]. Elham Dehghanpur Deharab, Peyvand Ghaderyan, Graphical representation and variability quantification of handwriting signals: New tools for Parkinson's disease detection, *Biocybernetics and Biomedical Engineering*, Volume 42, Issue 1, 2022, Pages 158-172, ISSN 0208-5216, <https://doi.org/10.1016/j.bbe.2021.12.007>.
- [14]. Claudio De Stefano, Francesco Fontanella, Donato Impedovo, Giuseppe Pirlo, Alessandra Scotto di Freca, Handwriting analysis to support neurodegenerative diseases diagnosis: A review, *Pattern Recognition Letters*, Volume 121, 2019, Pages 37-45, ISSN 0167-8655, <https://doi.org/10.1016/j.patrec.2018.05.013>.
- [15]. Shirin Salimi, Muireann Irish, David Foxe, John R. Hodges, Olivier Piguet, James R. Burrell, Can visuospatial measures improve the diagnosis of Alzheimer's disease?, *Alzheimer's & Dementia: Diagnosis, Assessment & Disease Monitoring*, Volume 10, 2018, Pages 66-74, ISSN 2352-8729, <https://doi.org/10.1016/j.dadm.2017.10.004>.
- [16]. Bai S, Liu W, Guan Y. The Visuospatial and Sensorimotor Functions of Posterior Parietal Cortex in Drawing Tasks: A Review[J]. *Frontiers in Aging Neuroscience*, 2021. DOI:10.3389/fnagi.2021.717002.
- [17]. Shimada Y, Meguro K, Kasai M, et al. Necker cube copying ability in normal elderly and Alzheimer's disease. A community-based study: The Tajiri project[J]. *Psychogeriatrics*, 2006. DOI:10.1111/j.1479-8301.2006.00121.
- [18]. Andrew J. Larner, Alex J. Mitchell, A meta-analysis of the accuracy of the Addenbrooke's Cognitive Examination (ACE) and the Addenbrooke's Cognitive Examination-Revised (ACE-R) in the detection of dementia, *International Psychogeriatrics*, Volume 26, Issue 4, 2014, Pages 555-563, ISSN 1041-6102, <https://doi.org/10.1017/S1041610213002329>.
- [19]. Kazuya Kawabata, Reiko Ohdake, Hirohisa Watanabe, Epifanio Bagarinao, Kazuhiro Hara, Aya Ogura, Michihito Masuda, Toshiyasu Kato, Takamasa Yokoi, Masahisa Katsuno, Gen Sobue, Visuo-perceptual disturbances in Parkinson's disease, *Clinical Parkinsonism & Related Disorders*, Volume 3, 2020, 100036, ISSN 2590-1125, <https://doi.org/10.1016/j.prdoa.2020.100036>.
- [20]. Juan Guerrero-Martín, María del Carmen Díaz-Mardomingo, Sara García-Herranz, Rafael Martínez Tomás, Mariano Rincón, A benchmark for Rey-Osterrieth complex figure test automatic scoring, *Heliyon*, Volume 10, Issue 21, 2024, e39883, ISSN 2405-8440, <https://doi.org/10.1016/j.heliyon.2024.e39883>.
- [21]. Sudhakar Hallur, Anil Gavade, Image feature extraction techniques: A comprehensive review, *Franklin Open*, Volume 12, 2025, 100366, ISSN 2773-1863, <https://doi.org/10.1016/j.fraope.2025.100366>.
- [22]. Bernardo, Lucas Salvador, et al. "A hybrid two-stage SqueezeNet and support vector machine system for Parkinson's disease detection based on handwritten spiral patterns" *International Journal of Applied Mathematics and Computer Science*, vol. 31, no. 4, University of Zielona Góra, 2021, pp. 549-561. <https://doi.org/10.34768/amcs-2021-0037>

- [23].Pakize Erdogmus, Abdullah Talha Kabakus, The promise of convolutional neural networks for the early diagnosis of the Alzheimer's disease, Engineering Applications of Artificial Intelligence, Volume 123, Part A, 2023, 106254, ISSN 0952-1976, <https://doi.org/10.1016/j.engappai.2023.106254>.
- [24].Wahiba Ismaiel, Lilia kechiche, Yassine Aribi, Omer Salih Dawood Omer, Walied Merghani, Leveraging edge detection techniques to enhance Arabic sign language static-gesture recognition using deep learning, Journal of Engineering Research,2025,ISSN 2307-1877,<https://doi.org/10.1016/j.jer.2025.09.011>.
- [25].Emanuele Nardone, Claudio De Stefano, Nicole Dalia Cilia, Francesco Fontanella, Handwriting strokes as biomarkers for Alzheimer's disease prediction: A novel machine learning approach, Computers in Biology and Medicine, Volume 190,2025,110039,ISSN 0010-4825,<https://doi.org/10.1016/j.compbiomed.2025.110039>.
- [26].Elli Valla, Sven Nömm, Kadri Medijainen, Pille Tabä, Aaro Toomela, Tremor-related feature engineering for machine learning based Parkinson's disease diagnostics, Biomedical Signal Processing and Control, Volume 75,2022,103551,ISSN 1746-8094,<https://doi.org/10.1016/j.bspc.2022.103551>.
- [27].C.D. Rios-Urrego, J.C. Vásquez-Correa, J.F. Vargas-Bonilla, E. Nöth, F. Lopera, J.R.Orozco-Arroyave, Analysis and evaluation of handwriting in patients with Parkinson's disease using kinematic, geometrical, and non-linear features, Computer Methods and Programs in Biomedicine, Volume 173,2019,Pages 43-52,ISSN 0169-2607,<https://doi.org/10.1016/j.cmpb.2019.03.005>.
- [28].Chenbin Ma, Yulan Ma, Longsheng Pan, Xuemei Li, Chunyu Yin, Rui Zong, Zhengbo Zhang, Automatic diagnosis of multi-task in essential tremor: Dynamic handwriting analysis using multi-modal fusion neural network, Future Generation Computer Systems, Volume 145, 2023, Pages 429-441, ISSN 0167-739X, <https://doi.org/10.1016/j.future.2023.03.033>.
- [29].Nicole D. Cilia, Giuseppe De Gregorio, Claudio De Stefano, Francesco Fontanella, Angelo Marcelli, Antonio Parziale, Diagnosing Alzheimer's disease from on-line handwriting: A novel dataset and performance benchmarking, Engineering Applications of Artificial Intelligence, Volume 111,2022,104822,ISSN 0952-1976,<https://doi.org/10.1016/j.engappai.2022.104822>.
- [30].Xuechao Wang, Jun qing Huang, Marianna Chatzakou, Sven Nömm, Elli Valla, Kadri, Medijainen, Pille Tabä, Aaro Toomela, Michael Ruzhansky, Comparison of one- two- and three-dimensional CNN models for drawing-test-based diagnostics of the Parkinson's disease, Biomedical Signal Processing and Control, Volume 87, Part B,2024,105436,ISSN 1746-8094,<https://doi.org/10.1016/j.bspc.2023.105436>.
- [31].Moises Diaz, Momina Moetesum, Imran Siddiqi, Gennaro Vessio, Sequence-based dynamic handwriting analysis for Parkinson's disease detection with one dimensional convolutions and BiGRUs, Expert Systems with Applications, Volume 168,2021,114405,ISSN 0957-4174,<https://doi.org/10.1016/j.eswa.2020.114405>.
- [32].Chenbin Ma, Peng Zhang, Long sheng Pan, Xuemei Li, Chunyu Yin, Ailing Li, Rui Zong, Zhengbo Zhang, A feature fusion sequence learning approach for quantitative analysis of tremor symptoms based on digital handwriting, Expert Systems with Applications, Volume 203,2022,117400,ISSN 0957-4174,<https://doi.org/10.1016/j.eswa.2022.117400>.
- [33].Vidhya R, Banavath D, S. Kayalvili Swarna Mahesh Naidu V. Charles Prabu D. Sugumar R. Hemalatha S. Vimal R. G. Vidhya. Alzheimer's disease detection using residual neural network with



- LSTM hybrid deep learning models[J].Journal of Intelligent & Fuzzy Systems: Applications in Engineering and Technology, 2023, 45(6):12095-12109.
- [34].Xuechao Wang, Jun qing Huang, Marianna Chatzakou, Kadri Medijainen, Aaro Toomela, Sven Nõmm, Michael Ruzhansky, LSTM-CNN: An efficient diagnostic network for Parkinson's disease utilizing dynamic handwriting analysis, Computer Methods and Programs in Biomedicine, Volume 247, 2024, 108066, ISSN0169-2607 , <https://doi.org/10.1016/j.cmpb.2024.108066>.
- [35].Hao Zhou, Liyong Yin, Rui Su, Ying Zhang, Yi Yuan, Ping Xie, Xin Li, STCGRU: A hybrid model based on CNN and BiGRU for mild cognitive impairment diagnosis, Computer Methods and Programs in Biomedicine, Volume 248, 2024, 108123, ISSN 0169-2607, <https://doi.org/10.1016/j.cmpb.2024.108123>.
- [36].Zhou Y , Gao C , Zhang X ,et al. Early Detection and Intervention of Alzheimer's disease Based on Game APP[J].2024 5th International Conference on Information Science, Parallel and Distributed Systems (ISPDS), 2024:182-188. DOI:10.1109/ispds62779.2024.10667634.
- [37].T. Wu, C. Gao, S. Wan, Y. Liu, X. Sun and Y. Zhao, "Fuzzy Evaluation Method of DPDFS for Unity Game Based Brain Training toward Prevention of AD," 2022 4th International Conference on Intelligent Control, Measurement and Signal Processing (ICMSP), Hangzhou, China, 2022, pp. 956-959, doi: 10.1109/ICMSP55950.2022.9859185.
- [38].Wahyuningsih T , Henderi H , Winarno W . Text Mining an Automatic Short Answer Grading (ASAG), Comparison of Three Methods of Cosine Similarity, Jaccard Similarity and Dice's Coefficient[J].Journal of Applied Data Sciences, 2021. DOI:10.47738/JADS.V2I2.31.
- [39].Zhou P, Shi W, Tian J, et al. Attention-Based Bidirectional Long Short-Term Memory Networks for Relation Classification[J]. 2016. DOI:10.18653/v1/P16-2034.
- [40].Linchao Zhang, Lei Hang, Research on the application of attention mechanism based multi-model fusion in food recommendation platforms, Engineering Applications of Artificial Intelligence, Volume 162, Part B, 2025, 112449, ISSN 0952-1976, <https://doi.org/10.1016/j.engappai.2025.112449>.
- [41].Huanhuan Gong, Yanying Li, Jiaoni Zhang, Baoshuang Zhang, Xialin Wang,A new filter feature selection algorithm for classification task by ensembling pearson correlation coefficient and mutual information, Engineering Applications of Artificial Intelligence, Volume 131,2024,107865,ISSN 0952-1976,<https://doi.org/10.1016/j.engappai.2024.107865>.
- [42].Galaz Z, Mekyska J, Mucha J, et al. Prodromal Diagnosis of Lewy Body Diseases Based on the Assessment of Graphomotor and Handwriting Difficulties[C]//arXiv.arXiv, 2023.DOI:10.48550/arXiv.2301.08534.